The Squaric Acid Derivatives $C_8O_4S_2$ and $C_8O_4Se_2$ – Crystal Structures, Explosive Thermal Behavior and the Preparation of Carbon Suboxide Selenide OC_3Se by Flash Vacuum Pyrolysis

Johannes Beck[a], Petra Krieger-Beck[a], and Klemens Kelm[b]

[a] Institute for Inorganic Chemistry, Rheinische Friedrich-Wilhelms-Universität Bonn, Gerhard-Domagk-Str. 1, D-53121 Bonn, Germany
[b] Institute for Inorganic Chemistry, Section for Inorganic Materials Research, Rheinische Friedrich-Wilhelms-Universität Bonn, Römerstr. 164, D-53117 Bonn, Germany

Reprint requests to Prof. Dr. Johannes Beck. Fax +49 (0)228 / 735660. E-mail: j.beck@uni-bonn.de

Z. Naturforsch. **61b,** 123 – 132 (2006); received September 19, 2005

2,7-Diselenatricyclo[6.2.0.0^{3,6}]deca-1,3-diene-4,5,9,10-tetraone, $C_8O_4Se_2$, was prepared from 1,2-diselenosquarate and squaric acid dichloride. Its crystal structure and the structure of the already known sulfur analogue $C_8O_4S_2$ were determined ($C_8O_4S_2$: orthorhombic, $Pca2_1$, $a = 1413.64(2)$, $b = 599.850(9)$, $c = 968.8(1)$ pm; $C_8O_4Se_2$: orthorhombic, $Pnnm$, $a = 415.46(2)$, $b = 894.29(5)$, $c = 1160.14(7)$ pm). The structures are not isotypic and show a different packing of the molecules whose symmetry deviate only slightly from D_{2h}. In the four-membered C_4 rings the C–C bonds represent one single bond, one double bond and two slightly shortened single bonds. The C_4 rings are thus to be considered as cyclobutene-dione fragments. The vigorous exothermic decomposition of the compounds that occurs on heating to 220 to 240 °C shows that both are energetic materials. The explosions are accompanied by a heat evolution of −192 kJ/mol for $C_8O_4S_2$ and −224 kJ/mol for $C_8O_4Se_2$. Performing the decomposition of $C_8O_4S_2$ in a closed autoclave leaves a residue of the composition "C_6S" which was examined by transmission electron microscopy techniques and shown to consist mainly of amorphous carbon. This thermal behaviour is limiting the utilization of $C_8O_4S_2$ and $C_8O_4Se_2$ as precursors for the syntheses of OC_3S and the yet unknown OC_3Se *via* FVP. The formation of OC_3S could be proven by the reaction of the trapped, slightly yellow product (evaporation at 200 °C, pyrolysis at 500 °C, trapping at −196 °C) with aniline which yielded thiomalonic acid dianilide, of which the crystal structure was determined (monoclinic, $C2/c$, $a = 2814.8(16)$, $b = 1201.7(8)$, $c = 809.2(4)$ pm, $\beta = 91.88(4)°$, $V = 2736(3) \cdot 10^6$ pm^3). The mass spectrum of $C_8O_4Se_2$ shows the strongest signal for OC_3Se^+, and FVP experiments (evaporation at 220 °C, pyrolysis at 650 °C, trapping at −75 °C) yielded small amounts of a bright yellow material which rapidly converted into a black polymer.

Key words: Squaric Acid Derivatives, Energetic Materials, Amorphous Carbon, Carbon Suboxide Selenide, Flash Vacuum Pyrolysis

Introduction

Chalcogenocumulenes of the general structure E=(C$_n$)=E with E = O, S and $n = 1-7$ form linear molecules and have received considerable interest since some of these molecules have been detected in carbon rich interstellar clouds [1]. In the condensed phase molecules of this class with more than one carbon atom have a pronounced tendency to polymerise. Under forcing conditions even the representatives with $n = 1$ are transformed to polymers. CS_2 yields a black polymer upon the action of high pressure [2], and a high-pressure modification of CO_2 with a SiO_2-type structure is known [3]. Thus only CO_2, CS_2, and OCS are stable at low pressure in the liquid and the solid state, while for example carbon suboxide OC_3O is long known to be rapidly transformed to a dark coloured polymer [4]. The same holds for carbonsubsulfide SC_3S, which is completely converted at ambient temperature within some hours from a red liquid to a dark-brown polymer [5]. The structures of these carbon rich solids are generally unknown, mostly due to their amorphous nature. For some time the carbonsuboxide polymer $(C_3O_2)_x$ was the object of structural studies and recently, substantial insight into the structure of this amorphous poly-

Table 1. Crystal data and details of data collection and refinement of $C_8O_4S_2$ (**3**), $C_8O_4Se_2$ (**4**) and $C_{15}H_{14}N_2OS$ (**5**).

Formula	$C_8O_4S_2$ (**3**)	$C_8O_4Se_2$ (**4**)	$C_{15}H_{14}N_2OS$ (**5**)
Crystal system, space group	orthorhombic, $Pca2_1$	orthorhombic, $Pnnm$	monoclinic, $C2/c$
Unit cell dimensions/pm	$a = 1413.6(2)$ $b = 599.85(9)$ $c = 968.8(1)$	$a = 415.46(2)$ $b = 894.29(5)$ $c = 1160.14(7)$	$a = 2814.8(16)$ $b = 1201.7(8)$ $c = 809.2(4)$ $\beta = 91.88(4)$
Unit cell volume/10^6pm^3	821.5	431.0	2735.8
Number of formula units	$Z = 4$	$Z = 2$	$Z = 8$
ρ_{calcd}/g·cm^{-3}	1.813	2.450	1.313
Absorption coefficient μ/cm^{-1}	6.3 (Mo-K$_\alpha$)	85.6 (Mo-K$_\alpha$)	2.3 (Mo-K$_\alpha$)
Range of data collection	$2\theta < 59.8^\circ$	$2\theta < 54.9^\circ$	$2\theta < 59.9^\circ$
Number of measured reflections	8920	3832	10927
Number of independent reflections, R_{int}	2384, 0.046	513, 0.046	3953, 0.086
Number of reflections in least squares	2384	513	3953
Number of refined parameters	129	35	216
$wR(F^2)$	0.078	0.049	0.102
$R(F)$ for [number] of reflections with $I > 4\sigma(F)$	0.035 [1781]	0.019 [451]	0.049 [1633]
Residual electron density/e/10^6pm^3	+0.25 / −0.25	+0.46 / −0.31	+0.19 / −0.20
Flack *x* parameter	0.61(1)	–	–

mer could be achieved by small angle scattering [6] and ^{13}C solid state NMR spectroscopy on ^{13}C enriched samples [7].

A prime prerequisite for further studies of the polymeric heterocumulenes is a synthetic procedure that allows for the synthesis of gram quantities. For OC_3O synthetic routes are known that fulfil this condition. The dehydration of malonic acid [4] or the cleavage of $(H_3C)_3SiOH$ from malonic acid bis(trimethylsilyl)ester [8] can be used to obtain OC_3O on a 10 g scale. For the other chalcogenocumulenes, especially the sulfur containing OC_3S and SC_3S, no such advantageous syntheses are known [9]. In the last decades chalcogenocumulenes have been prepared from suitable molecular precursors by flash vacuum pyrolysis (FVP) or photolysis. A large number of thio- and oxocumulenes have been characterized, for example exotic molecules as the nine-atomic OC_7O from melithic acid anhydride [10] or ethene-1,2-dithione, SC_2S, with an unusual electronic ground state structure [11]. The reactive species were trapped in an argon matrix and identified spectroscopically. The fragmentation of several sulfur containing heterocycles by FVP and mass spectrometry has been studied [12 – 14]. The occurrence of the desired molecular fragments in the mass spectra is generally indicative of a successful FVP process.

Our goal was to find preparative routes to carbon suboxide sulfide, OC_3S (**1**), and the unknown carbon suboxide selenide, OC_3Se (**2**), which allow for the preparation of gram quantities. The reported synthesis of **1** by repeated contact of gaseous, moisturized

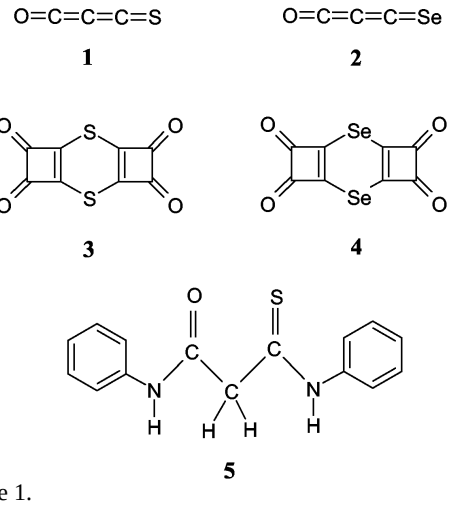

Scheme 1.

OC_3O with solid P_4S_{10} [15] yields quantities sufficient for vibrational spectroscopic investigations, but seems not to be suitable for expansion to the preparative scale. On the other hand, flash vacuum pyrolysis has already been successfully applied and the well-known heterotricycle $C_8O_4S_2$ (**3**) was described to be appropriate for evaporation and subsequent pyrolysis to yield **1** [16].

Here we report on the crystal structure of **3**, the synthesis and crystal structure of its selenium analogue **4**, on our attempts to prepare **1** and **2** on a preparative scale *via* FVP of **3** and **4**, respectively, the remarkable thermal properties of **3** and **4** as the limiting factors for pyrolysis experiments, the crystal structure of the aniline adduct of **1** and a transmission electron micro-

scope investigation of the carbonaceous residue of the thermal decomposition of **3**.

Experimental Section

Squaric acid, squaric acid dibutylester and triphenylarsine were purchased (ALDRICH) and used as obtained. Squaric acid dichloride $C_4O_2Cl_2$ was obtained from squaric acid and $SOCl_2$ [17]. $C_8O_4S_2$ (**3**) was synthesized from squaric acid dichloride, H_2S, and triphenylarsine as described [16, 18]. ^{13}C NMR (300 MHz, CD_3CN, +60 °C): 186.6 ppm (C=O), 183.8 ppm (C=C).

For the flash-vacuum-pyrolysis processes an apparatus as depicted in [16] with continuous evacuation was used. Behind the pyrolysis oven three subsequent cold traps with −20 °C, −75 °C, and −196 °C were installed.

Sodium 1,2-diselenosquarate, $Na_2(C_4O_2Se_2)$. Al_2Se_3 was prepared by melting a thoroughly powdered mixture of Al powder and grey selenium. The mixture was added in small portions into a porcelain crucible, which was flushed with Ar. After the first portion was ignited with a small piece of burning Mg, the reaction proceeded vigorously on adding the following portions. After reaching ambient temperature, the dark coloured Al_2Se_3 was finely powdered and used for the preparation of H_2Se by dropwise addition of aqueous H_2SO_4 under Ar. The H_2Se/Ar gas mixture was bubbled through a solution of NaOEt in dry ethanol. NaHSe was obtained by this way as a slightly pink powder which was filtered off under Ar and stored in a glove box under Ar. In an analogous procedure as described for the synthesis of dithiosquarate(2–) [19], NaHSe and squaric acid dibutylester were refluxed for 30 min in dry ethanol. Sodium 1,2-diselenosquarate $Na_2(C_4O_2Se_2)$ [20] precipitated as a light yellow powder, which was filtered off and dried in a vacuum.

2,7-Diselenatricyclo[6.2.0.0^{3,6}]deca-1,3-diene-4,5,9,10-tetraone (**4**). To a stirred suspension of 3.0 g (0.016 mol) of vacuum dried $Na_2(C_4O_2Se_2)$ in 150 ml of CH_2Cl_2 a solution of 1.6 g (0.016 mol) squaric acid dichloride in 50 ml CH_2Cl_2 was added dropwise at ambient temperature. After stirring for two hours 250 ml H_2O was added to the reaction mixture. An orange powder precipitated from the organic phase. The two phases were separated and the organic phase was filtered. After concentration by distilling off three quarters of the solvent a second crop of **4** was obtained. Overall yield 3.3 g = 65%. IR(KBr) ν = 1760(vs), 1720(s), 1442(s), 1132(s), 1050(s), 900(w), 840(m), 788(w), 742(m), 477(s) cm^{-1} – ^{13}C NMR (300 MHz, CD_3CN, +60 °C): 186.7 ppm (C=O), 186.3 ppm (C=C) – MS(EI): *m/z* (%) = 316 – 322 (30) [M^+], 292 (10) [M^+–CO], 182 (30) [$Se_2C_2]^+$, 131 (100) [OC_3Se^+].

Monothiomalonic dianilide (**5**). 3 g of **3** was placed in the quartz tube of an FVP apparatus. In the evaporation zone the temperature was set to 200 °C and in the pyrolysis zone to 500 °C. After 5 h heating was terminated. In the −75 °C cold trap small amounts of a slightly yellow solid had deposited. 10 ml of CH_2Cl_2 were added. To 2 ml of this solution an excess of a saturated solution of aniline in hexane was added which caused the immediate precipitation of 30 mg of colourless crystalline **5** which was filtered off and dissolved in THF. Slow diffusion by layering of this solution with hexane gave colourless crystals of m.p. 141 °C. IR(KBr) ν = 3220(s), 3125(m), 3040(m), 1646(s), 1632(s), 1592(s), 1542(s), 1497(s), 1443(m), 1415(s), 1339(m), 1307(w), 1276(m), 1220(m), 1175(w), 1142(w), 1119(m), 1072(w), 1024(w), 981(w), 948(w), 905(m), 850(m), 799(m), 781(m),

Table 2. Fractional atomic coordinates and equivalent isotropic Debye-Waller factor $U_{equiv}/10^2$ pm^2 for the atoms in the structures of $C_8O_4S_2$ (**3**), $C_8O_4Se_2$ (**4**) and $C_{15}H_{14}N_2OS$ (**5**). Standard deviations given in brackets refer to the last significant digits.

Atom	*x*	*y*	*z*	U_{equiv}
$C_8O_4S_2$ (**3**)				
S1	0.18826(4)	0.48914(10)	0.39150(8)	4.78(2)
S2	0.08387(4)	−0.01811(9)	0.24201(7)	4.01(2)
O1	−0.13279(14)	0.1399(4)	0.4087(3)	6.79(6)
O2	−0.04296(16)	0.5994(4)	0.5360(2)	7.50(7)
O3	0.31426(16)	−0.1131(4)	0.0876(3)	8.05(8)
O4	0.40303(13)	0.3401(3)	0.2223(2)	5.75(5)
C1	0.07455(16)	0.3802(4)	0.3990(3)	3.99(5)
C2	0.03710(16)	0.1906(4)	0.3444(2)	3.52(5)
C3	−0.05817(16)	0.2331(5)	0.4051(3)	4.64(6)
C4	−0.01616(19)	0.4479(5)	0.4667(3)	5.23(8)
C5	0.23320(16)	0.2841(4)	0.2838(2)	3.53(5)
C6	0.19510(14)	0.0972(4)	0.2290(3)	3.49(5)
C7	0.28617(18)	0.0338(5)	0.1581(3)	4.85(7)
C8	0.32865(16)	0.2466(4)	0.2216(3)	4.21(6)
$C_8O_4Se_2$ (**4**)				
Se	0.24842(6)	0.68671(3)	0	2.78(2)
O	0.2874(4)	0.6541(3)	−0.31774(17)	5.17(5)
C1	0.4134(5)	0.5645(2)	−0.11767(15)	2.54(4)
C2	0.4005(6)	0.5727(2)	−0.24666(15)	3.13(5)
$C_{15}H_{14}N_2OS$ (**5**)				
S	0.79250(2)	0.07068(5)	0.39655(9)	5.58(2)
O	0.69297(5)	−0.12285(11)	0.56977(18)	3.98(4)
N1	0.82019(6)	−0.14168(15)	0.4125(2)	3.93(4)
N2	0.67408(6)	0.00844(15)	0.3784(2)	4.01(5)
C1	0.73905(7)	−0.11580(19)	0.3259(3)	3.82(5)
C2	0.78652(7)	−0.06575(17)	0.3832(2)	3.65(5)
C3	0.69963(6)	−0.07717(17)	0.4348(3)	3.30(4)
C11	0.86937(7)	−0.12727(17)	0.4568(3)	3.87(5)
C12	0.90078(8)	−0.20243(19)	0.3914(3)	4.80(6)
C13	0.94860(9)	−0.1960(2)	0.4345(4)	5.54(7)
C14	0.96511(9)	−0.1163(2)	0.5428(3)	5.64(7)
C15	0.93384(9)	−0.0424(2)	0.6081(3)	5.67(7)
C16	0.88588(8)	−0.0474(2)	0.5672(3)	4.89(6)
C21	0.63724(7)	0.06128(17)	0.4674(3)	3.56(5)
C22	0.64169(9)	0.17208(19)	0.5077(3)	5.00(6)
C23	0.60612(10)	0.2248(2)	0.5906(4)	6.38(8)
C24	0.56682(10)	0.1677(3)	0.6326(4)	6.64(8)
C25	0.56208(8)	0.0572(3)	0.5940(3)	6.18(7)

Table 3. Selected distances /pm and angles /° in the structures of $C_8O_4S_2$ (**3**), $C_8O_4Se_2$ (**4**) and $C_{15}H_{14}N_2OS$ (**5**).

$C_8O_4S_2$ (**3**)			
Distances			
S1 – C5	173.3(2)	C1 – C2	136.1(3)
S1 – C1	173.7(3)	C1 – C4	149.6(3)
S2 – C6	172.2(2)	C2 – C3	149.1(3)
S2 – C2	172.9(2)	C3 – C4	153.9(4)
O1 – C3	119.4(3)	C5 – C6	135.2(3)
O2 – C4	119.2(3)	C5 – C8	149.5(3)
O3 – C7	118.3(3)	C6 – C7	150.8(3)
O4 – C8	119.2(3)	C7 – C8	153.9(4)
Angles			
C5 – S1 – C1	95.6(1)	C1 – C4 – C3	86.2(2)
C6 – S2 – C2	95.8(1)	C6 – C5 – C8	94.4(2)
C2 – C1 – C4	93.7(2)	C5 – C6 – C7	92.8(2)
C1 – C2 – C3	93.2(2)	C6 – C7 – C8	86.7(2)
C2 – C3 – C4	87.0(2)	C5 – C8 – C7	86.2(2)
$C_8O_4Se_2$ (**4**)			
Distances			
Se – C1	187.8(2)	C1 – C2	149.9(2)
O – C2	119.6(3)	C2 – $C2^{I}$	154.1(4)
C1 – $C1^{I}$	136.0(4)		
Angles			
C1 – Se – $C1^{II}$	93.2(1)	C2 – C1 – Se	133.2(2)
C2 – C1 – $C1^{I}$	93.5(1)	$C2^{I}$ – C2 – C1	86.5(2)
C^{1} – C1 – Se	133.4(1)		
$C_{15}H_{14}N_2OS$ (**5**)			
Distances			
C2 - S	165.1(2)	C1 – C2	152.4(3)
C3 - O	124.2(2)	C1 – C3	151.2(3)
C2 – N1	133.1(3)	N1 – C11	142.9(3)
C3 – N2	132.7(3)	N2 – C21	143.1(3)
Angles			
C11 – N1 – C2	129.8(2)	N1 – C2 –S	126.8(2)
C21 – N2 – C3	124.4(2)	C1 – C2 – S	119.9(2)
C1 – C2 – N1	113.3(2)	C1 – C3 – O	120.8(2)
C1 – C3 – N2	116.0(2)	N2 – C3 – O	123.3(2)
C2 – C1 – C3	110.8(2)		

751(s), 723(s), 699(s), 689(s), 615(w), 608(w), 569(m), 524(m), 501(m), 470(m) cm^{-1} – ^{1}H NMR (300 MHz, THF-d_8): 11.4 (s, 1H, NH), 9.6 (s, 1H, NH), 8-7 (m, 10 H, Ph), 3.9 (s, 2H, CH_2) – ^{13}C NMR (300 MHz, THF-d_8): 194.0 (C=S), 166.6 (C=O), 140.2 – 119.7 (8 signals, arom.), 54.8 (CH_2).

Crystal structure determinations

Single crystals of compounds $C_8O_4S_2$ (**3**) and $C_8O_4Se_2$ (**4**) were grown from saturated CH_3CN solutions, crystals of thiomalonic dianilide (**5**) from a saturated THF solution upon slow diffusion of hexane. The crystal quality for X-ray diffraction was checked by preliminary precession photographs. Data sets were recorded at ambient temperature with a Nonius CAD4 diffractometer for **3** and **5** and a Bruker-Nonius Kappa-CCD diffractometer for **4**, both equipped with monochromatized Mo-K_α radiation. Lattice symmetries and space groups were derived from simulated images of the reciprocal lattice. Structures were solved using direct methods (SHELXS-97 [21]) and refined on F^2 with anisotropic displacement parameters for all atoms (SHELXL-97 [22]). The structure of **3** turned out to be non-centrosymmetric in the space group $Pca2_1$. An inversion twinning with a volume ratio 0.6/0.4 of the two individuals had to be included in the refinement. An empirical absorption correction was applied to the data set of **4**, a numerical absorption correction to the data set of **5**. The hydrogen atoms in the structure of **5** were refined with individual positional parameters but with a common isotropic displacement parameter. Table 1 contains the crystal data and details of structure refinement, Table 2 the positional parameters and Table 3 selected bond lengths and angles.

Crystallographic data for the crystal structures have been deposited with the Cambridge Crystallographic Data Centre, 12 Union Road, Cambridge CB2 1EZ, UK, (Fax: int.code+(1223)336-033; e-mail for inquiry: fileserv @ccdc.cam.ac.uk) from where they can be obtained by quoting the depository numbers CCDC-284263 for **3**, CCDC-284264 for **4** and CCDC-284265 for **5**.

Transmission electron microscopy

Two transmission electron microscopes were used for this study: A Philips CM 30 ST equipped with an electron energy loss spectrometer (Gatan PEELS 666) and a Philips CM 300 UT FEG equipped with a Gatan Imaging Filter (GIF). Both microscopes were operated at 300 keV. Samples for transmission electron microscopy (TEM) were prepared by grinding the dry material in an agate mortar. Subsequently, the powder was applied to a holey carbon film supported by a copper TEM grid (Quantifoil).

Results and Discussion

The selenium containing analogue **4** of the well known squaric acid based heterocyclic system **3** can be obtained from squaric acid dichloride and sodium-1,2-diselenosquarate as an orange crystalline powder. The colour is only slightly darker in comparison with the sulfur analogue. **4** has only limited solubility in usual organic solvents. Only very polar solvents like CH_3CN, CH_3NO_2 or DMF allow for the preparations of concentrated solutions. The ^{13}C NMR spectrum was therefore recorded in CD_3CN, but only at an elevated temperature of 60 °C the concentration was high enough to achieve substantial resonance intensities. The observed two resonances, as already reported

for **3** [19], are in line with the highly symmetric D_{2h} structure.

*Crystal structures of $C_8O_4S_2$ (**3**) and $C_8O_4Se_2$ (**4**)*

The crystal structures of the compounds $C_8O_4S_2$ (**3**) and $C_8O_4Se_2$ (**4**) consist of almost planar, isomorphous molecules, but are crystallographically not isotypic. Molecules **3** have no crystallographic symmetry, while molecules **4** have $2/m$ symmetry with a mirror plane perpendicular to the molecular plane through both selenium atoms Se and Se^I and a twofold axis in the molecular plane bisecting the four C–C bonds C2–$C2^I$, C1–$C1^I$, $C1^{II}$–$C1^{III}$, and $C2^{II}$–$C2^{III}$. All molecules are essentially planar with the largest deviations from the best plane through all 14 atoms for **3** at 5.2 pm for S1 and 3.8 pm for O2, and for **4** at only 1.1 pm for Se and Se^I. Thus both molecules almost fulfil the ideal D_{2h} symmetry (Figs 1 and 2). The four-membered C_4 rings deviate strongly from a square structure and are distorted to trapezoids. The bonds C1–C2 (136 pm) and C5–C6 (135 pm) for **3** and C1-$C1^I$, $C1^{II}$–$C1^{III}$ (136 pm) for **4** represent C=C double bonds, the bonds C3–C4 (154 pm) and C7–C8 (154 pm) for **3** and C2–$C2^I$, $C2^{II}$–$C2^{III}$ (154 pm) for **4** C–C single bonds. C1–C4 (150 pm), C2–C3 (149 pm), C5–C8 (150 pm), and C6–C7 (151 pm) for **3** and C1–C2, $C1^I$–$C2^I$, $C1^{II}$–$C2^{II}$, $C1^{III}$–$C2^{III}$ (150 pm) for **4** represent slightly shortened single bonds. These bond length distributions indicate, that in the structures of **3** and **4** aromatic delocalisation as found in the highly symmetric squarate anions $C_4O_4^{2-}$ is not present and the four membered rings are cyclobutenedione systems. The C–S bonds (in average 173 pm) and C–Se bonds (188 pm) represent single bonds and

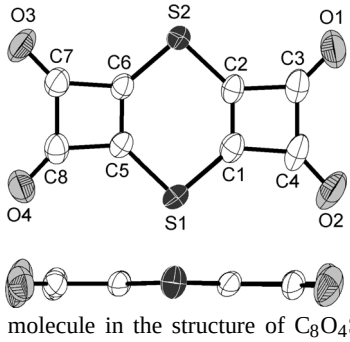

Fig. 1. The molecule in the structure of $C_8O_4S_2$ (**3**) from two different points of view. On top a view perpendicular to the molecular plane, on bottom a view along the S1–S2 axis showing the almost complete planarity. Thermal ellipsoides are scaled to enclose a 50% probability.

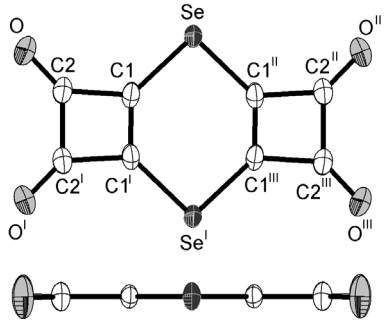

Fig. 2. The molecule in the structure of $C_8O_4Se_2$ (**4**). Two views are shown, on top perpendicular to the molecular plane, on bottom along the Se–Se^I axis showing the planarity of the molecule. Thermal ellipsoides are scaled to enclose a 50% probability.

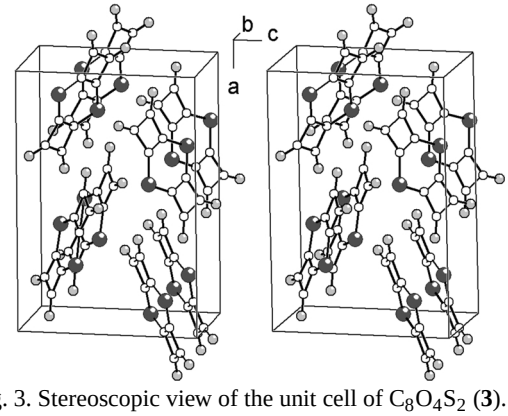

Fig. 3. Stereoscopic view of the unit cell of $C_8O_4S_2$ (**3**).

can be compared with C–S in S,S'-diphenyl-1,2-dithiosquarate (171 pm, [23]) and C–Se in dinaphto-1,4-diselenine-tetraone (190 pm [24]), and are significantly longer than for typical thioketones (160 pm [25]) or selenoketones (177 pm [26]). Molecules with 1,4-dithiine rings (the middle ring of **3**) can occur in a planar shape or bent along the axis through the two sulfur atoms. The bent molecular shape is observed more often than the planar one, but the energy difference between the two forms is generally very small [27]. The same holds for 1,4-diselenines. Up to now five molecules have been structurally characterized bearing six-membered Se_2C_4 rings of which two are planar and three are bent [28]. Both, **3** and **4**, belong to the respective planar class.

The packing of the molecules in the structures of **3** and **4** is different (Figs 3 and 4). In the structure of **4** two different orientations of the molecules are present, while in the structure of **3** four different orientations are found. The molecules of **4** are all colinearly ori-

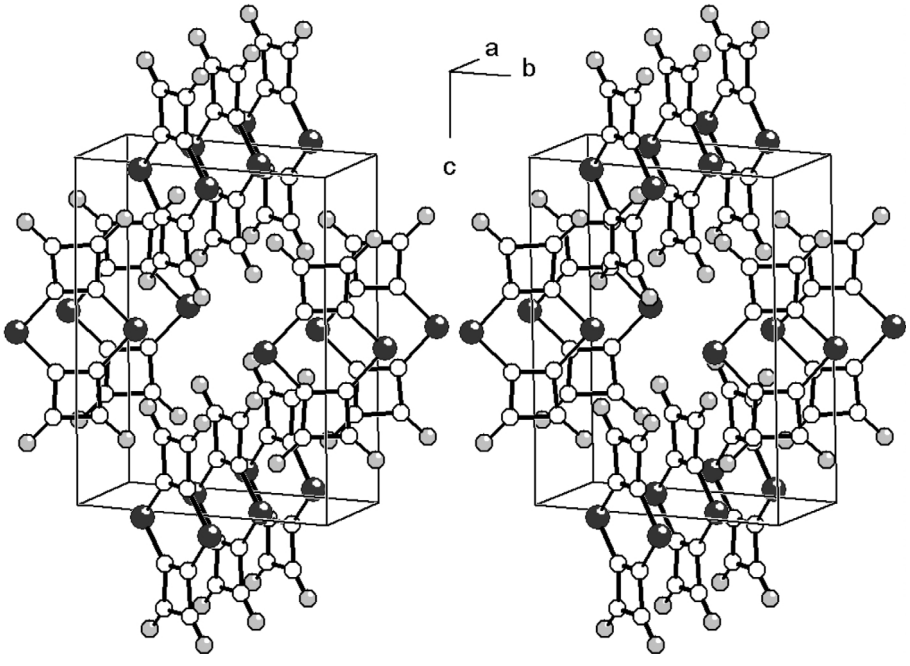

Fig. 4. Stereoscopic view of the unit cell of $C_8O_4Se_2$ (**4**).

ented in the direction of the crystallographic *c* axis. The different packing in the two structures can be understood by reducing the structures to the packing of the centres of gravity of the molecules. In the structure of **3** the molecules are arranged in a packing related to that of black phosphorus, while in the structure of **4** the molecules are arranged in the motif of a distorted cubic closest packing. In both structures stacks of mutually parallel molecules can be distinguished. The distances between the planes of nearest neighbors are 305 pm for **3** and 351 pm for **4**. The molecules are strongly shifted against each other and therefore, despite the short stacking distances, π-π interactions may not be important.

*Thermal behaviour of $C_8O_4S_2$ (**3**) and $C_8O_4Se_2$ (**4**)*

For **3** melting points with decomposition of 165 °C [19] and 174 °C [18] were reported. Actually, pure recrystallized and carefully dried samples of **3** do not show melting in this temperature region. If samples of **3** are heated with 5 °C/min between 215 and 225 °C, a vigorous decomposition with an explosive noise and the eruptive evolution of black powdery material is observed. **4** shows an analogous behaviour in the temperature range between 230 and 240 °C. The decomposition of **4** is visually and acoustically more violent than that of **3**. These unexpected effects were investigated by differential scanning calorimetry (DSC). In closed Al crucibles samples of both compounds were heated up to 240 °C with 0.5 °C/min. Up to 190 °C for **3** and 180 °C for **4** no thermal effects were detected. With onset temperatures of 207 °C for **3** and 195 °C for **4** strong and sharp exothermic signals appeared which correspond to decomposition enthalpies of −192 kJ/mol for **3** and −224 kJ/mol for **4**. Both compounds are therefore energetic materials.

To follow the stoichiometry of the explosive decomposition process, the residue of the decomposition of **3** was investigated. For this purpose, a 0.5 g sample of **3** was placed in a steel autoclave, which was installed in a preheated furnace at 300 °C. After one hour the autoclave was taken out of the oven, cooled to ambient temperature and opened. 0.22 g of a voluminous black material was obtained, which gave an analysis of 70.5% C and 29.3% S, corresponding to a formula "$C_{6.4}S$". A thermogravimetric analysis of this residue showed a first mass loss of 13.9% at temperatures between 100 and 220 °C and a second mass loss of 17.5% in the high temperature region between 600 and 1100 °C, in total 31.4%. The complete loss of all sulfur from "$C_{6.4}S$" would require a mass loss of 29.4%. The temperature for the first mass loss is quite low and one can assume that CS_2 is the leaving species. In contrast the temper-

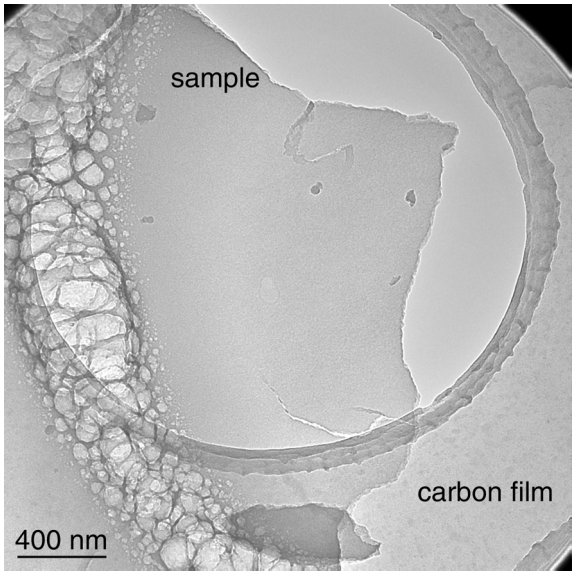

Fig. 5. TEM image of the decomposition product of **3**.

ature for the second mass loss is very high. Probably sulfur covalenty bound within a carbon-sulfur network is slowly liberated.

To gain further insight into the nature of this carbon rich material, a transmission electron microsopic study was untertaken. The material consisted of flakes of thin, self supporting films combined with regions with a foam like appearance (Fig. 5). No diffraction contrast was present in the bright field images. Furthermore, in diffraction mode no discrete reflections but diffuse halos were observed. This proves the material to be amorphous.

To clarify the nature of the carbon as well as the sulfur present, the energy loss near edge structure (ELNES) of the carbon K-edge was recorded. Spectra were taken on the CM 300 microscope (diffraction coupled, dispersion 0.2 eV/channel, illumination angle 5 mrad, acceptance angle 21 mrad). Two typical spectra of film-like regions are shown in Fig. 6. The background of the spectra was subtracted and the plural scattering was removed. The only prominent feature present in the ELNES is a prepeak at 284 eV, usually attributed to a π-π* transition in amorphous carbon [29]. For comparison, a spectrum of the holey carbon film of the TEM grid is also given (Fig. 6). The spectra are essentially identical while other carbon modifications exhibit pronounced fine structured ELNES [29]. Despite the fact that the material contains significant amounts of sulfur, we conclude the carbon

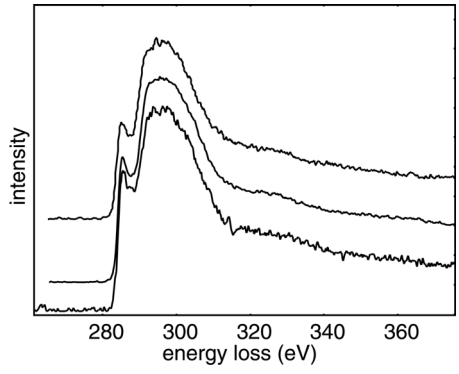

Fig. 6. ELNES of the carbon K-edge of the decomposition product of **3** (bottom and middle spectra) and an amorphous carbon film (top spectrum).

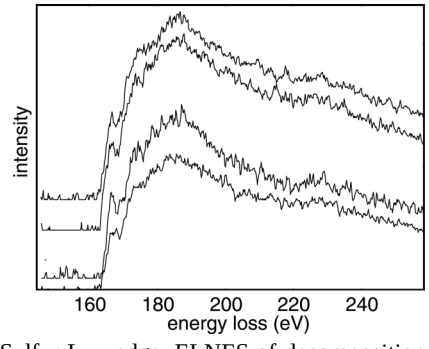

Fig. 7. Sulfur $L_{2,3}$-edge, ELNES of decomposition product of **3**. Individual spectra were recorded at different locations on the samples.

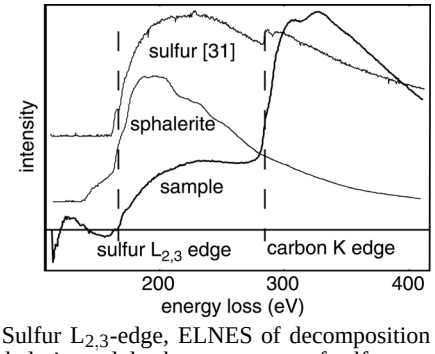

Fig. 8 Sulfur $L_{2,3}$-edge, ELNES of decomposition product of **3**, sphalerite and database spectrum of sulfur.

fraction of the residue of **3** to be principally similar to amorphous carbon.

Spectra of the sulfur $L_{2,3}$-edge were also recorded using the same conditions as for carbon. Again, an ELNES showing only a few prominent features was observed (Fig. 7). In contrast to this observation, an intensely structured ELNES has been reported for sev-

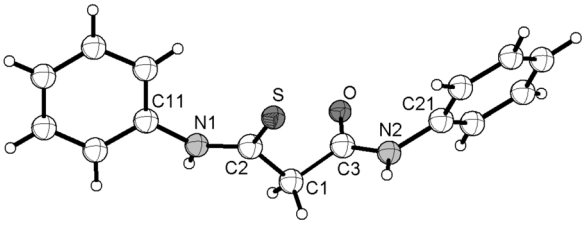

Fig. 9. The molecule in the structure of monothiomalonic acid dianilide (**5**), $H_5C_6N(H)C(O)C(H_2)C(S)N(H)C_6H_5$. Thermal ellipsoides are scaled to enclose a 50% probability. H atoms are drawn with an arbitrary radius.

eral inorganic sulfides and sulfates [30]. This is further illustrated in Fig. 8, where a spectrum of the residual from **3**, zinc sulfide (sphalerite) and a database spectrum of elemental sulfur [31] are reproduced (CM 30, diffraction coupled, dispersion 1 eV/channel, illumination angle 1 mrad, collection angle 13.5 mrad, background subtracted). While the difference in ELNES between sphalerite and the decomposition product is evident, there is only a small difference in the ELNES of sulfur and the residue of **3**, indicating a similar electronic structure. Unfortunately, there is a lack of adequate spectra of carbon-sulfur compounds for comparison, so no further information can be extracted from the measured $L_{2,3}$ ELNES.

*FVP experiments and mass spectrum of $C_8O_4Se_2$ (**4**)*

The fragmentation of $C_8O_4S_2$ (**3**) by pyrolysis has already been studied. **3** has been reported to decompose at 370 °C to give CO and OC_3S (**1**), of which the photoelectron and mass spectra [16] and the infrared and microwave spectra were measured [32]. On repeating the pyrolytic decomposition of **3** by evaporation at 200 °C and subsequent pyrolysis at 500 °C we found this procedure not suitable for the synthesis of gram quantities of **1**. The volatility of **3** is low and at elevated temperatures of > 200 °C slow decomposition occurs, followed by explosion above 220 °C [33]. By keeping a 3 g sample of **3** at 200 °C for several hours only about 50 mg of **1** could be obtained. Our observations are in line with the results of Maier and Ruppel, who, however, reported the total failure of this pyrolysis experiment [43, 44]. Attemps to improve the yield of **1** by applying a gas flow of He (1 – 20 l/min, He pressures 2 – 50 mbar) through the pyrolysis tube in order to bring larger quantities of evaporated **3** into the pyrolysis zone, were unsucessful.

In order to prove the formation of **1** and to test for the yield of the decomposition product we used the reaction with aniline which immediately generated monothiomalonic dianilide **5**. This compound is already known and the synthesis from acetylacetic acid anilide and phenylisocyanate has been described [36], but its crystal structure was unknown.

It crystallizes in the monoclinic crystal system with eight molecules in the unit cell. The remarkable structural features of the molecule are two essentially planar subunits (Fig. 9). The first one is made up by the atoms C1/C2/S/N1/H3/C11 with the highest deviation of 2.6 pm for C11, the second one is made up by C1/C3/O/N2/H4/C21 with the highest deviation of 3.5 pm for N2. The interplanar angle of 76.4 ° shows the carbonyl and the thiocarbonyl group to be in a *gauche* conformation. The bonds N1–C2 and N2–C3 (averaged 133 pm) are remarkably short, while the attached C=O (124 pm) and the C=S (165 pm) bonds are slightly elongated. Bond lengths and angles around the central methylene carbon atom C1 are as expected (C–C averaged 152 pm, C–C–C and H–C–H 111°). The structural parameters of **5** are very close to those of monothiomalonic amide, of which the *cis* and *trans* form have been structurally investigated [37].

The mass spectrum of **4** (Fig. 10) shows features closely related to the fragmentation pattern of **3** with its strong M^+ signal at $m/z = 224$, minor signals for $C_3S_2{}^+$ at $m/z = 100$ and $C_2S_2{}^+$ at $m/z = 88$, and the predominant signal at $m/z = 84$ for OC_3S^+. The mass spectrum of **4** is dominated by three fragments, M^+ ($m/z = 320$), $C_2Se_2{}^+$ ($m/z = 184$), and OC_3Se^+ ($m/z = 132$). This assignment can be made unequivocally on the basis of simulations of the isotopic patterns of the respective signals (Fig. 10). The predominant signal of OC_3Se^+ gives rise to hope for the synthesis of carbon suboxide selenide **2** by a pyrolysis experiment. Evaporating **4** at 200 °C and pyrolysis of the vapour at 650 °C gave small amounts of a bright yellow compound in the −75 °C cold trap. All attempts to purify this material by destillation into a −196 °C cold trap failed. On warming to temperatures above −10 °C the yellow colour disappeared and a black non-volatile residue was formed probably due to polymerzation. To confirm the synthesis of **2** by this method further work will be necessary which, however, seems to be lucrative to obtain further knowledge on the properties of this unknown compound.

Acknowledgements

The support of this work within the *Sonderforschungsbereich 408* (Collaborative Research Centre) of the *Deutsche Forschungsgemeinschaft* (German Research Council) is

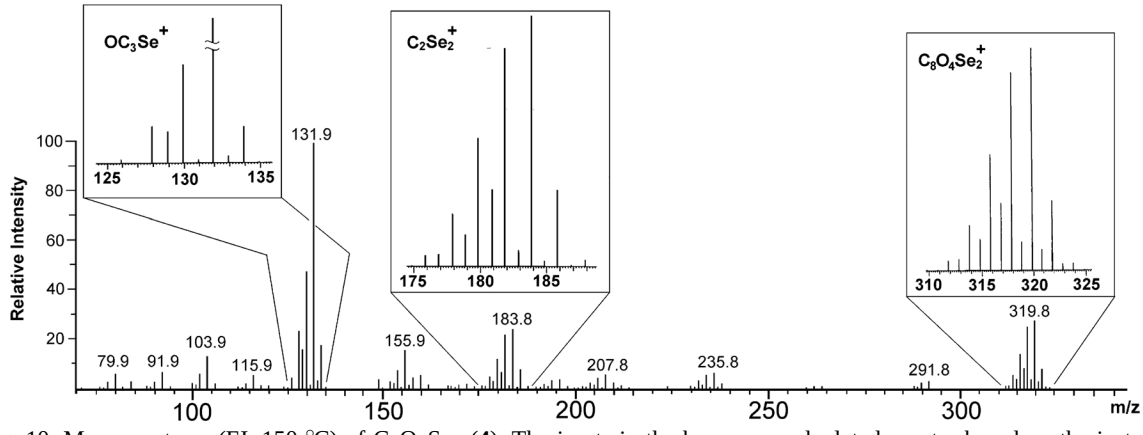

Fig. 10. Mass spectrum (EI, 150 °C) of $C_8O_4Se_2$ (**4**). The insets in the boxes are calculated spectra based on the isotopic distribution of C, O and Se, respectively.

gratefully acknowledged. We thank K. Armbruster for the preparation of NaHSe, J. Daniels and A. Roloff for the diffraction data collection.

[1] E. Herbst, Ann. Rev. Phys. Chem. **46**, 27 (1995); T. M. Leen, M. M. Graff, Astrophys. J. **325**, 411 (1988).
[2] P. W. Bridgeman, Proc. Am. Acad., Arts Sci. **74**, 339 (1941).
[3] V. Iota, C. S. Yoo, H. Cynn, Science **283**, 1510 (1999).
[4] O. Diels, B. Wolf, Ber. Dtsch. Chem. Ges. **39**, 689 (1906).
[5] B. v. Lengyel, Ber. Dtsch. Chem. Ges. **26**, 2960 (1893).
[6] M. Ballauff, L. Li, S. Rosenfeldt, N. Dingenouts, J. Beck, P. Krieger-Beck, Angew. Chem. **116**, 5967 (2004); Angew. Chem. Int. Ed. **43**, 5843 (2004).
[7] J. Schmedt auf der Günne, J. Beck, W. Hoffbauer, P. Krieger-Beck, Chem. Eur. J. **11**, 4429 (2004).
[8] L. Birkofer, P. Sommer, Chem. Ber. **109**, 1701 (1976).
[9] W. Stadlbauer, T. Kappe, Sulfur Reports **21**, 423 (1999).
[10] G. Maier, H. P. Reisenauer, A. Ulrich, Tetrahedron Lett. **32**, 4469 (1991).
[11] G. Maier, H. R. Reisenauer, J. Schrot, R. Janoschek, Angew. Chem. **102**, 1475 (1990); Angew. Chem. Int. Ed. **29**, 1464 (1990).
[12] D. Suelzle, J. K. Terlouw, H. Schwarz, J. Am. Chem. Soc. **112**, 628 (1990).
[13] D. Suelzle, H. Schwarz, J. Am. Chem. Soc. **113**, 48 (1991).
[14] C. Th. Pedersen, R. Flammang, P. Gerbaux, E. Fanghänel, J. Chem. Soc. Perkin Trans. 2, 1403 (1998).
[15] M. Winnewisser, J. Christiansen, J. Chem. Phys. Lett. **37**, 270 (1976).
[16] H. Bock, R. Dammel, D. Jaculi, J. Am. Chem. Soc. **108**, 7844 (1986).
[17] R. C. De Selms, C. J. Fox, R. C. Riordan, Tetrahedron Lett. 781 (1970).
[18] A. H. Schmidt, A. Aimène, M. Hoch, Synthesis 754 (1984).
[19] G. Seitz, K. Mann, R. Schmiedel, R. Matusch, Chem. Ber. **112**, 990 (1979).
[20] U. Drutkowski, B. Wenzel, P. Strauch, Inorg. Chem. Comm. **1**, 449 (1988).
[21] G. M. Sheldrick, SHELXS-97, Program for Crystal Structure Solution, University of Göttingen, Germany (1997).
[22] G. M. Sheldrick, SHELXL-97, Program for Crystal Structure Refinement, University of Göttingen, Germany (1997).
[23] U. Azzena, S. Cossu, O. DeLucchi, G. Valle, Acta Crystallogr. **C45**, 604 (1989).
[24] E. Ahsbahs, J. Ehlers, G. Klar, J. Chem. Res. **184**, 1383 (1992).
[25] C. D. Shirell, D. E. Williams, Acta Crystallogr. **B29**, 2128 (1973).
[26] P. R. Brooks, J. A. Counter, A. R. Bishop, E. R. T. Tiekink, Acta Crystallogr. **C47**, 1939 (1991).
[27] J. Beck, J. Weber, A. B. Mukhopadhyay, M. Dolg, New J. Chem. **29**, 465 (2005).
[28] Cambridge Crystallographic Database (CSD, version 5.26, release Nov 2004).
[29] S. D. Berger, D. R. McKenzie, P. J. Martin, Phil. Mag. Lett. **57**, 285 (1988).
[30] C. C. Calvert, A. J. Scott, R. Brydson, D. A. Banks, G. E. Lloyd, PEELS Studies of the Sulfur $L_{2,3}$ and Metal $L_{2,3}$-ELNES in Sulfur Bearing Minerals, in:

Electron microscopy and analysis: Proceedings of the Institute of Physics Electron Microscopy and Analysis Group conference, Inst. Phys. Conf. Ser. No.161, Section 5, p. 199, London, Institute of Physics (1999).
[31] EL/P 3.0, Gatan Cooperation, Pleasentown, CA, Core Loss Atlas (1994).
[32] M. Winnewisser, E. W. Peau, Acta. Phys. Hung. **55**, 33 (1984).
[33] Explosive decomposition of **3** on applying too high temperatures did in no case cause bursting of the quartz tube since the vacuum pump with a volume capacity of 4.3 m^3/h was able to pump off the evolved gases. This shows that the thermal decomposition of **3** is not detonative but rather a smooth explosion.
[34] R. Ruppel, Ph. D. Thesis, University of Giessen, Germany (1999).
[35] G. Maier, H. P. Reisenauer, R. Ruppel, Eur. J. Org. Chem. 4197 (2004).
[36] G. Barnikow, J. Prakt. Chem. **34**, 251 (1966).
[37] S. De Beukeleer, G. S. Papaefstathiou, C. P. Raptopoulou, A. Terzis, S. P. Perlepes, H. O. Desseyn, E. Manessi-Zoupa, Z. Naturforsch. **57b**, 1224 (2002).